AAS 16-410

AUTONOMOUS GUIDANCE ALGORITHM FOR MULTIPLE SPACECRAFT AND FORMATION RECONFIGURATION MANEUVERS

Theodore Wahl,[*] and Kathleen Howell[†]

Spacecraft formations operating autonomously have the potential to support a wide variety of missions. In this investigation, the creation of an autonomous guidance algorithm is explored for a formation reconfiguration maneuver involving an arbitrary number of spacecraft. The assessment process to construct a maneuver is decomposed into 2 problems: assignment and delivery. The guidance algorithm employs an auction process to assign each spacecraft a position in the formation. The guidance algorithm then uses Adaptive Artificial Potential Functions (AAPFs) to deliver each spacecraft to its target position. Ultimately, the guidance strategy requires from the user only the initial targets' states to complete the reconfiguration maneuvers.

INTRODUCTION

The operation of satellites or spacecraft in formations is an important development that may allow new civilian and military operational capabilities. NASA's Terrestrial Planet Finder (TPF), ESA's Darwin, and the Air Force Research Laboratory's TechSat-21 are some mission concepts which previously explored the utility of formation flying.[1–3] Examples of recent operational missions include the German-Swedish Prisma mission which is a formation flying technology demonstration mission involving two spacecraft, and NASA's Magnetospheric Multiscale (MMS) mission, which employs four spacecraft, operating in conjunction, to investigate Earth's magnetosphere.[4,5] Spacecraft formations are typically investigated for mission scenarios that cannot be accomplished by a single vehicle; additionally, cooperating formations can potentially be more robust and adaptable than single, monolithic spacecraft. However, multiple spacecraft operating in close proximity introduce additional complexities into the guidance system that do not appear in single spacecraft missions. For example, formation reconfiguration maneuvers are employed when multiple spacecraft are guided simultaneously to different positions within the formation. The solution to such a problem is essentially a multi-step operation since each spacecraft must be assigned a target position and each vehicle is then guided into its new position. To operate efficiently and quickly in such environments, autonomous guidance and control algorithms are a key necessity for the successful implementation of these types of maneuvers. A decentralized autonomous guidance algorithm for formation maneuvers is the focus of this investigation.

[*]Ph.D. Student, School of Aeronautics and Astronautics, Purdue University, 701 West Stadium Avenue, West Lafayette, IN 47907-2045

[†]Hsu Lo Distinguished Professor of Aeronautics and Astronautics, School of Aeronautics and Astronautics, Purdue University, 701 West Stadium Avenue, West Lafayette, IN 47907-2045

For the development of this formation guidance system two specific problems are identified. First, the "assignment problem" involves assigning the spacecraft in the formation to their new target positions. A satisfying solution to the assignment problem fills all the positions in the formation; a desirable solution fills all the positions such that the propellant usage is minimized. An auction algorithm is introduced to address the assignment problem. Auction algorithms are a well accepted method of solving the classical assignment problem, which is matching n spacecraft and n target positions.[6] There is some benefit for every combination of spacecraft and target, and each target carries a price. A spacecraft's "satisfaction" with its assignment is based on the trade-off between benefit and price. Through a simple algorithm, the target prices are raised as the different spacecraft bid on the targets that yield the greatest satisfaction. The algorithm terminates when all the spacecraft are sufficiently satisfied with their assigned target.

The second task in any reconfiguration problem is the "delivery problem," that is, guiding each spacecraft to its assigned position. Any guidance strategy that supports a formation of vehicles operating autonomously must be sufficiently simple in terms of the onboard computational requirements while still offering accurate and propellant-efficient relative trajectory computations and delivery. Simultaneously, the complexity involving multiple vehicles in the likely operational environment implies continually evolving relative motions yet includes constraints on both the path and time. Thus, with awareness of such limits, but also with efficiency and accuracy as priorities, the proposed guidance strategy is based on Artificial Potential Functions (APF). Artificial potential functions offer simple mathematical guidance laws that are implemented in real time and do not require any a priori assumptions concerning the system dynamics.[7]

The problem is introduced with a brief initial overview of the equations of orbital relative motion and the structure of the formations used as examples for the guidance algorithm. This guidance strategy is designed for a nonlinear regime and the simulations do not rely on any linearized dynamics. The guidance algorithm's solution to the delivery problem is then introduced. The mathematical descriptions of the artificial potential functions employed in the algorithm are summarized along with examples of their performance in guiding a single spacecraft. Then, the auction process to solve the assignment problem is detailed. The classic auction is first introduced, and then the modifications to improve the auction's performance for spacecraft operations are added. Finally, demonstrations of the guidance algorithm and the reconfiguration maneuvers are assessed.

BACKGROUND: RELATIVE MOTION

For a formation of spacecraft, accurately modeling the relative motion is a necessity for a guidance strategy. To represent the relative motion of spacecraft orbiting Earth, the Hill or Local-Vertical Local-Horizontal (LVLH) frame is used. The Hill frame is a reference frame attached to a spacecraft as it orbits the Earth. For a formation, one spacecraft can be designated the "Chief" while the others are denoted as "Deputies." Alternatively, it is not required that the Chief be a physical vehicle, rather it may exist simply as a reference orbit for the formation. The Chief's motion serves as the basis for the definition of the Hill frame with the Chief located at the origin. The $\hat{x}$ direction is then aligned with the radius vector directed from Earth's center toward the Chief, the $\hat{z}$ direction is aligned with the Chief's orbital angular momentum vector, and $\hat{y}$ is formed from $\hat{y} = \hat{z} \times \hat{x}$. If the Chief moves in a circular orbit, the $\hat{y}$ direction is aligned with the in-track velocity direction.

To derive the dynamical equations for relative motion in the Hill frame, the positions and velocities are defined relative to the Chief; each spacecraft position relative to the Chief in the Hill frame is represented by the vector $\boldsymbol{\rho} = x\hat{x} + y\hat{y} + z\hat{z}$. In the Earth Centered Inertial (ECI) frame, the

position of the Chief with respect to the Earth center is defined by $\mathbf{r_c}$. Similarly, the position of a Deputy in the ECI frame is denoted by $\mathbf{r_d}$. Rewriting the position of the Chief in the ECI frame, $\mathbf{r_c}$, as a Hill frame vector yields: $\mathbf{r_c} = r_c\hat{x}$, where r_i is the magnitude of $\mathbf{r_i}$. Written in terms of Hill frame coordinates, $\mathbf{r_d}$ is:

$$\mathbf{r_d} = \mathbf{r_c} + \boldsymbol{\rho} = (r_c + x)\hat{x} + y\hat{y} + z\hat{z} \tag{1}$$

The inertial second derivative of $\mathbf{r_d}$ with respect to time, is then:

$$\ddot{\mathbf{r_d}} = (\ddot{r_c} + \ddot{x} - \ddot{\theta_c}y - 2\dot{\theta_c}\dot{y} - \dot{\theta_c}^2(r_c + x))\hat{x} + (\ddot{y} + \ddot{\theta_c}(r_c + x) + 2\dot{\theta_c}(\dot{r_c} + \dot{x}) - \dot{\theta_c}^2 y)\hat{y} + \ddot{z}\hat{z} \tag{2}$$

where θ_c is the true anomaly of the Chief orbit and $\dot{\theta_c}$ is its rate of change. The scalar rate of change of $\mathbf{r_c}$ is denoted $\dot{r_c}$. The second derivative of $\mathbf{r_c}$ in the Hill frame is then:

$$\ddot{\mathbf{r_c}} = (\ddot{r_c} - \dot{\theta_c}^2 r_c)\hat{x} + (\ddot{\theta_c}r_c + 2\dot{\theta_c}\dot{r_c})\hat{y} \tag{3}$$

Assuming the only force acting on the spacecraft is the force of gravity due to a spherically symmetric Earth gravity field, with the gravitational parameter of Earth represented by μ, the inverse-square acceleration on the Chief is represented by:

$$\ddot{\mathbf{r_c}} = -\frac{\mu}{r_c^2}\hat{x} \tag{4}$$

Equating the components of Eq. (3) and Eq. (4) yields:

$$\ddot{r_c} = \dot{\theta_c}^2 r_c - \frac{\mu}{r_c^2} \tag{5}$$

$$\ddot{\theta_c} = -\frac{2\dot{\theta_c}\dot{r_c}}{r_c} \tag{6}$$

Now, Eq. (2) is re-written as:

$$\ddot{\mathbf{r_d}} = (\ddot{x} - \frac{\mu}{r_c^2} + 2\dot{\theta_c}(\frac{\dot{r_c}y}{r_c} - \dot{y}) - \dot{\theta_c}^2 x)\hat{x} + (\ddot{y} + 2\dot{\theta_c}(\dot{x} - \frac{\dot{r_c}x}{r_c}) - \dot{\theta_c}^2 y)\hat{y} + \ddot{z}\hat{z} \tag{7}$$

Again assuming a spherical Earth, the acceleration on the Deputy spacecraft in the Hill frame can be written as:

$$\ddot{\mathbf{r_d}} = -\frac{\mu}{r_d^3}(r_c + x)\hat{x} - \frac{\mu}{r_d^3}y\hat{y} - \frac{\mu}{r_d^3}z\hat{z} \tag{8}$$

Equating the components of Eq. (7) and Eq. (8) produces the familiar equations of motion for the Deputy spacecraft in the Hill frame:

$$\ddot{x} = \frac{\mu}{r_c^2} + \dot{\theta_c}^2 x - 2\dot{\theta_c}(\frac{\dot{r_c}y}{r_c} - \dot{y}) - \frac{\mu}{r_d^3}(r_c + x) \tag{9}$$

$$\ddot{y} = \dot{\theta_c}^2 y - 2\dot{\theta_c}(\dot{x} - \frac{\dot{r_c}x}{r_c}) - \frac{\mu}{r_d^3}y \tag{10}$$

$$\ddot{z} = -\frac{\mu}{r_d^3}z \tag{11}$$

Unless otherwise stated, these are the equations of motion for both the spacecraft and target vehicles in all simulations.

These nonlinear equations accurately describe the relative motion in the Hill frame for Keplerian orbits–that is, orbits around a spherically symmetric Earth. Additionally, there is no requirement on the orbit of the Chief in the derivation of these equations; thus, the differential equations are valid for Chief orbits of any eccentricity. The Hill frame is selected as the working frame for the guidance development because it better corresponds to the formation motion as viewed by a member spacecraft as opposed to an Earth centered inertial frame. Higher fidelity relative motion models, e.g., Earth's gravity zonal harmonics, and the influences of the Sun and Moon, are difficult to derive directly in the Hill frame, thus, such perturbed motion is propagated in an Earth centered inertial frame and the results converted into the Hill frame.

To avoid drifting apart, it is necessary that the relative motion of the vehicles within the formation remain bounded. A fundamental concept in formation flying is the matching of the orbital energies of the Deputy spacecraft with that of the Chief. The Chief's energy is represented as E_c and is evaluated from the Chief orbit semi-major axis, a_c:

$$E_c = -\frac{\mu}{2a_c} \tag{12}$$

The energy associated with the orbit of a Deputy is represented by E_d, and is defined as:

$$E_d = \frac{1}{2}\dot{r_d}^2 - \frac{\mu}{r_d} = \frac{1}{2}((\dot{x} - \dot{\theta}_c y + \dot{r_c})^2 + (\dot{y} + \dot{\theta}_c(x + r_c))^2 + \dot{z}^2) - \frac{\mu}{\sqrt{(r_c + x)^2 + y^2 + z^2}} \tag{13}$$

When these two energies are equated, the following relationship is produced:

$$\frac{1}{2}((\dot{x} - \dot{\theta}_c y + \dot{r_c})^2 + (\dot{y} + \dot{\theta}_c(x + r_c))^2 + \dot{z}^2) - \frac{\mu}{\sqrt{(r_c + x)^2 + y^2 + z^2}} = -\frac{\mu}{2a_c} \tag{14}$$

Matching orbital energy allows formations that are bounded. For a given Chief orbit, an initial Deputy position, $\boldsymbol{\rho}$, is selected and the relative velocity values are determined.

Figure 1 and Figure 2 demonstrate the motion, as observed in the Hill frame, of three spacecraft whose orbital energies have been matched. The Chief orbit for this simulation is defined with a perigee altitude of 1,000 km and an eccentricity equal to 0.05. To produce these closed curves in the Hill frame–also denoted natural motion circumnavigation (NMC)–all the initial relative velocity in Eq. (14) is pre-specified to be in the $\dot{y}$ component direction; i.e., $\dot{x} = 0$ and $\dot{z} = 0$. The motion of the Deputies are then periodic with the same period as the Chief orbit. Under perturbations, the relative motion is no longer exactly periodic, but an energy-matched formation experiences less relative drift than an non-energy-matched formation.[8]

DELIVERY

The delivery problem is defined as the path-planning process that allows each spacecraft to reach its assigned target in the formation while avoiding close approaches to any other spacecraft or obstacle. This second phase in the guidance algorithm is introduced prior to the first–i.e., assignment–phase because the mechanism to deliver the spacecraft to the targets clearly influences the assignments. There are numerous strategies for guiding a spacecraft to a target state, for example, model predictive control or sliding mode control. For this investigation, however, the solution to the delivery problem is based on artificial potential function guidance. As a guidance option, APFs provide a computationally simple scheme to guide a spacecraft to a target rendezvous with inherent obstacle avoidance properties. First, the mathematical formulation of traditional artificial potential functions is summarized; then, an extension to APFs, that is, Adaptive Artificial Potential Functions, is developed. The performance of APF and AAPF guidance is then demonstrated.

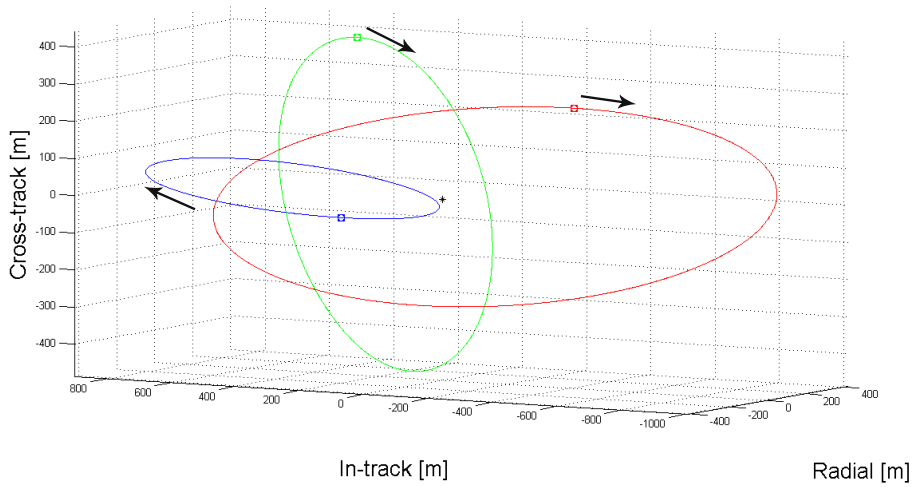

Figure 1. Trajectories for a formation of 3 spacecraft as viewed in the Hill frame. The initial and final positions are represented as circles and squares, respectively. The "Chief" is identified as an asterisk.

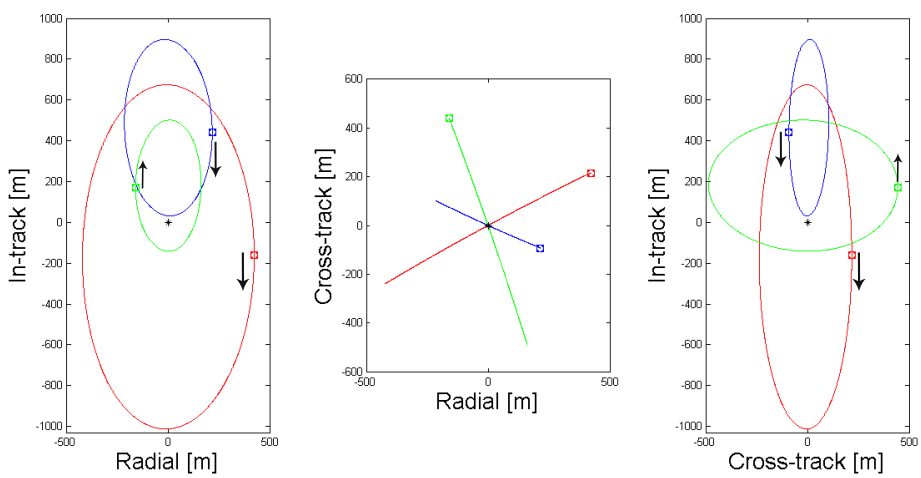

Figure 2. 2D projections of the trajectories in Figure 1.

Artificial Potential Functions

The motivation for artificial potential function guidance is robot motion planning with a methodology that links the kinematic planning problem with the dynamic execution problem in an appropriate manner.[7,9] Such a connection is accomplished by creating a potential function that incorporates the necessary freespace and goal information. The artificial potential function is structured such that the negative gradient of the potential leads to the desired target and avoids any obstacles. The minimum of the potential is placed at the target location, and obstacle locations are surrounded by areas of high potential.

To create a potential field with the minimum at the target and maximums surrounding the obstacles, the potential function is separated into attractive and repulsive pieces. The attractive potential function is typically a Lyapunov candidate function to ensure that the spacecraft approaches the target asymptotically. The attractive potential, ϕ_a, is a quadratic function based on the separation

between the spacecraft position in the Hill frame, $\boldsymbol{\rho}$, and the target position in the Hill frame, $\boldsymbol{\rho_t}$. It is described as follows:

$$\phi_a = \frac{k}{2} \left(\boldsymbol{\rho} - \boldsymbol{\rho_t}\right)' Q \left(\boldsymbol{\rho} - \boldsymbol{\rho_t}\right) \tag{15}$$

In this expression, k is a scalar weighting factor, selected by the user, and Q is a positive-definite matrix that describes the shape of the attractive potential. For the analysis using APF guidance, Q is defined as the identity matrix of order 3; the attractive potential is spherically symmetric. The construction of ϕ_a ensures the attractive potential is a Lyapunov function. The repulsive potential, ϕ_r, for a single obstacle is similarly described:

$$\phi_r = \frac{K}{2} \frac{\left(\boldsymbol{\rho} - \boldsymbol{\rho_t}\right)' Q \left(\boldsymbol{\rho} - \boldsymbol{\rho_t}\right)}{\left(\boldsymbol{\rho} - \boldsymbol{\rho_o}\right)' P \left(\boldsymbol{\rho} - \boldsymbol{\rho_o}\right) - 1} \tag{16}$$

Here, K is a scalar weighting factor, determined by the user, $\boldsymbol{\rho_o}$ is the position of the obstacle in the Hill frame, and P is a positive-definite matrix that describes the size and shape of an ellipsoid. The denominator in the repulsive potential is structured to create an ellipsoid of repulsion around the obstacle. This ellipsoid accommodates uncertainty in the obstacle position and shape. The numerator essentially contains the attractive potential–which ensures that the target position is at the minimum of the total potential–similar to the method described by Ge and Cui as well as Muñoz.[10,11] If there are multiple obstacles, the repulsive potential is a combination of the individual potentials. For example, if there are n obstacles, and $\boldsymbol{\rho_{o,i}}$ represents the position of the i-th obstacle in the Hill frame, the repulsive potential is:

$$\phi_r = \frac{K}{2} \sum_{i=1}^{n} \frac{\left(\boldsymbol{\rho} - \boldsymbol{\rho_t}\right)' Q \left(\boldsymbol{\rho} - \boldsymbol{\rho_t}\right)}{\left(\boldsymbol{\rho} - \boldsymbol{\rho_{o,i}}\right)' P \left(\boldsymbol{\rho} - \boldsymbol{\rho_{o,i}}\right) - 1} \tag{17}$$

For the later simulations, the only obstacles potentially in the path of each spacecraft are the other spacecraft in the formation. Marking the other spacecraft as obstacles prevents intra-formation collisions, however, it is also possible to include obstacles beyond the formation members which could represent debris or even other satellites.

The total potential is the sum of the attractive and repulsive portions: $\phi = \phi_a + \phi_r$. The desired velocity recommended by the APF guidance law, i.e., $\mathbf{v_d}$, is the negative gradient of the total potential:

$$\mathbf{v_d} = -\nabla\phi = -\nabla\phi_a - \nabla\phi_r \tag{18}$$

This desired velocity, $\mathbf{v_d}$, is the velocity as defined in the Hill frame, so it is a velocity with respect to the Chief. This desired velocity guides the spacecraft to the target location—provided the target is stationary. For a moving target, the spacecraft must match the target position and velocity to enable a rendezvous. The velocity matching is accomplished with a method similar to one used by Ge and Cui and by Muñoz: a simple velocity matching condition that is added to the APF calculation.[10,12]

To match the velocity vectors, the difference between the spacecraft and target velocities is combined with the desired velocity from the negative gradient of the potential function. Additionally, a velocity vector angle separation threshold determines if a maneuver is necessary. The Hill frame velocity vector of the spacecraft is represented by $\mathbf{v}$ and the target velocity vector by $\mathbf{v_t}$.

$$\mathbf{v} = \begin{bmatrix} \dot{x} \\ \dot{y} \\ \dot{z} \end{bmatrix} \tag{19}$$

An error in velocity, $\boldsymbol{\varepsilon_v}$, is defined as the difference between the spacecraft and target velocity vectors:

$$\boldsymbol{\varepsilon_v} = \mathbf{v} - \mathbf{v_t} \tag{20}$$

The angle, ψ, between $\boldsymbol{\varepsilon_v}$ and $\mathbf{v_d}$ is also defined:

$$\psi = \arccos\left(\frac{\boldsymbol{\varepsilon_v} \cdot \mathbf{v_d}}{|\mathbf{v_d}||\boldsymbol{\varepsilon_v}|}\right) \tag{21}$$

If ψ is larger than a user set threshold, $\psi \geq \psi^*$, then the APF guidance strategy recommends an impulsive $\mathbf{\Delta V}$, defined as the difference between $\mathbf{v_d}$ and $\boldsymbol{\varepsilon_v}$:

$$\mathbf{\Delta V} = \mathbf{v_d} - \boldsymbol{\varepsilon_v} \tag{22}$$

Again, this impulsive $\mathbf{\Delta V}$ is expressed in terms of Hill frame coordinates and is relative to the Chief. In this investigation, a threshold angle, ψ^* of 45° is employed throughout.

Artificial potential functions are mathematically simple and do not rely on any a priori dynamical assumptions to successfully guide spacecraft to target positions. This simplicity is attractive because it facilitates on-board operation–necessary for an autonomous guidance system. However, as is demonstrated in the next section, APF guidance of spacecraft can require a larger amount of maneuvering ΔV than is strictly necessary. To lower the magnitude of the total ΔV as a consequence of the maneuvers, the potential functions in the guidance algorithm are adapted to leverage the natural dynamics. This extension of the fundamental strategy is labeled adaptive artificial potential function guidance.

Adaptive Artificial Potential Functions

The development of Adaptive Artificial Potential Function guidance is described by Muñoz.[10] The goal involves the incorporation of the natural dynamics in shaping the potential functions for autonomous on-orbit maneuvers. For the rendezvous problem, Muñoz assumes relative dynamics consistent with the Clohessy-Wiltshire (CW) system which has the advantage of linearity due to a circular Chief orbit, but the principles still apply in the nonlinear relative motion system described in Eq. (9)-(11). The Adaptive Artificial Potential Function (AAPF) development begins with a two point boundary value problem in the linear system. In a linear system, the equations of motion of a spacecraft can be easily described using a State Transition Matrix (STM), $\Phi(t, t_0)$:

$$\begin{bmatrix} \boldsymbol{\rho} \\ \mathbf{v} \end{bmatrix} = \Phi(t, t_0) \begin{bmatrix} \boldsymbol{\rho_0} \\ \mathbf{v_0} \end{bmatrix} \tag{23}$$

Here, t_0 is the starting time, t is the current time, and $\boldsymbol{\rho_0}$ and $\mathbf{v_0}$ represent the initial position and initial velocity vectors of the spacecraft in the Hill frame. The STM in Muñoz's work is evaluated using the CW equations and the Chief circular orbit as a reference. For the nonlinear relative motion system in this investigation, the State Transition Matrix used in AAPF guidance is either created by numerical integration of the relative motion equations using the target as a reference or created with an analytical approximation using the Chief elliptical orbit as a reference. Similar to the spacecraft, in the linear system, the equations of motion of the target can be written as:

$$\begin{bmatrix} \boldsymbol{\rho_t} \\ \mathbf{v_t} \end{bmatrix} = \Phi(t, t_0) \begin{bmatrix} \boldsymbol{\rho_{t,0}} \\ \mathbf{v_{t,0}} \end{bmatrix} \tag{24}$$

Errors in position and velocity, $\mathbf{e_r}$ and $\mathbf{e_v}$, are then defined as the difference between the spacecraft and target states:

$$\begin{bmatrix}\mathbf{e_r}\\ \mathbf{e_v}\end{bmatrix} = \begin{bmatrix}\boldsymbol{\rho}-\boldsymbol{\rho_t}\\ \mathbf{v}-\mathbf{v_t}\end{bmatrix} = \Phi(t,t_0)\begin{bmatrix}\mathbf{e_{r,0}}\\ \mathbf{e_{v,0}}\end{bmatrix} \tag{25}$$

At the final time, t_f, the error in position, $\mathbf{e_r}$, should be zero. To match the spacecraft to the target final position, an impulsive $\mathbf{\Delta V}$ is applied to the error in velocity, $\mathbf{e_v}$, at the initial time, t_0.

$$\begin{bmatrix}\mathbf{e_r}\\ \mathbf{e_v}\end{bmatrix} = \begin{bmatrix}\Phi_{11}(t_f,t_0) & \Phi_{12}(t_f,t_0)\\ \Phi_{21}(t_f,t_0) & \Phi_{22}(t_f,t_0)\end{bmatrix}\begin{bmatrix}\mathbf{e_{r,0}}\\ \mathbf{e_{v,0}}+\mathbf{\Delta V}\end{bmatrix} \tag{26}$$

The top line yields a simple targeter when solved such that $\mathbf{e_r} = \mathbf{0}$

$$\mathbf{0} = \Phi_{11}(t_f,t_0)\mathbf{e_{r,0}} + \Phi_{12}(t_f,t_0)(\mathbf{e_{v,0}}+\mathbf{\Delta V}) \tag{27}$$

The $\mathbf{\Delta V}$ vector that solves the above equation is:

$$\mathbf{\Delta V} = -\Phi_{12}^{-1}(t_f,t_0)\Phi_{11}(t_f,t_0)\mathbf{e_{r,0}} - \mathbf{e_{v,0}} \tag{28}$$

In the linear variational system, this $\mathbf{\Delta V}$ will bring the spacecraft to the target's position by t_f. The goal of AAPF is to adapt the potential shape such that the gradient of the attractive potential follows the velocity profile supplied by the initial maneuver. With the appropriate substitution of Eq. (28) into Eq. (26) the error in velocity is predicted for any time, t, after this maneuver as:

$$\mathbf{e_v} = (\Phi_{21}(t,t_0) - \Phi_{22}(t,t_0)\Phi_{12}^{-1}(t_f,t_0)\Phi_{11}(t_f,t_0))\mathbf{e_{r,0}} \tag{29}$$

A feedback update for the potential shape is necessary, so the starting time, t_0, is shifted to the current time, t. This shift produces a simpler form for the error in velocity:

$$\mathbf{e_v} = -\Phi_{12}^{-1}(t_f,t)\Phi_{11}(t_f,t)\mathbf{e_r} \tag{30}$$

This error in velocity vector becomes the desired velocity profile, $\mathbf{v_d}$, with which the artificial potential function gradient is aligned. In application, the "final time", t_f, is updated at every time step and is expressed as a function of the current time: $t_f = t + \tau$. The time τ is denoted the "look-ahead time", and is selected by the operator to advance t_f.

To adapt the potential function to the desired velocity profile in Eq. (30), the shape factor, Q, is considered as a time varying matrix, $Q(t)$, and it includes the weighting information formerly represented by k. To maintain the benefits of a symmetric positive-definite shaping matrix, a Cholesky factorization is performed on $Q(t)$:

$$Q(t) = R(t)^T R(t) \tag{31}$$

where the Cholesky factor, $R(t)$, is the upper right triangular matrix:

$$R(t) = \begin{bmatrix} q_{11}(t) & q_{12}(t) & q_{13}(t)\\ 0 & q_{22}(t) & q_{23}(t)\\ 0 & 0 & q_{33}(t)\end{bmatrix} \tag{32}$$

Now, the attractive potential is written as:

$$\phi_a = \frac{1}{2}\mathbf{e_r}'R(t)^T R(t)\mathbf{e_r} \tag{33}$$

A new error variable, $\boldsymbol{\varepsilon}$, is introduced as the difference between the desired velocity, $\mathbf{v_d}$, and the negative gradient of the attractive potential:

$$\boldsymbol{\varepsilon} = \mathbf{v_d} - (-\nabla\phi_a) \tag{34}$$

This error variable is re-written in terms of the error position, STM, and $R(t)$ as:

$$\boldsymbol{\varepsilon} = -\Phi_{12}^{-1}(t_f,t)\Phi_{11}(t_f,t)\mathbf{e_r} + R(t)^T R(t)\mathbf{e_r} \tag{35}$$

The elements of $R(t)$ are determined to drive $\boldsymbol{\varepsilon}$ to zero, by setting $\dot{\boldsymbol{\varepsilon}} = -\boldsymbol{\varepsilon}$. The time derivative, $\dot{\boldsymbol{\varepsilon}}$, is evaluated as:

$$\dot{\boldsymbol{\varepsilon}} = -\Phi_{12}^{-1}(t_f,t)\Phi_{11}(t_f,t)\mathbf{e_v} + R(t)^T R(t)\mathbf{e_v} + Y\dot{\mathbf{q}} \tag{36}$$

Here, $\mathbf{q}$ is a vector of the Cholesky factors described in Eq. (32):

$$\mathbf{q} = \begin{bmatrix} q_{11} \\ q_{12} \\ q_{13} \\ q_{22} \\ q_{23} \\ q_{33} \end{bmatrix} \tag{37}$$

and Y is a matrix comprised of the Cholesky factor elements and the error position elements:

$$Y^T = \begin{bmatrix} (2q_{11}e_{r1} + q_{12}e_{r2} + q_{13}e_{r3}) & q_{12}e_{r1} & q_{13}e_{r1} \\ q_{11}e_{r2} & (q_{11}e_{r1} + 2q_{12}e_{r2} + q_{13}e_{r3}) & q_{13}e_{r2} \\ q_{11}e_{r3} & q_{12}e_{r3} & (q_{11}e_{r1} + q_{12}e_{r2} + 2q_{13}e_{r3}) \\ 0 & (2q_{22}e_{r2} + q_{23}e_{r3}) & q_{23}e_{r2} \\ 0 & q_{22}e_{r3} & (q_{22}e_{r2} + 2q_{23}e_{r3}) \\ 0 & 0 & 2q_{33}e_{r3} \end{bmatrix} \tag{38}$$

When $\dot{\boldsymbol{\varepsilon}} = -\boldsymbol{\varepsilon}$, it is possible to solve for $\dot{\mathbf{q}}$, that is:

$$\dot{\mathbf{q}} = Y^T(YY^T)^{-1}[\Phi_{12}^{-1}(t_f,t)\Phi_{11}(t_f,t)\mathbf{e_v} - R(t)^T R(t)\mathbf{e_v} - \boldsymbol{\varepsilon}] \tag{39}$$

Once the six scalar differential equations in Eq. (39) are numerically integrated, the Cholesky factor, R, is created from the elements of $\mathbf{q}$ as ordered in Eq. (32). From R, the new attractive potential shaping matrix, Q, is formed as in Eq. (31). The initial condition for the integration is the Cholesky factorization of a 3x3 identity matrix. With Q established, the AAPF guidance procedure is identical to the APF method described previously.

As previously noted, AAPF guidance was first developed for use under the assumption of linear dynamics.[10] The Clohessy-Wiltshire equations offer an analytical approximation of relative motion in the Hill frame for a circular Chief orbit, and an STM constructed for the CW equations completely describe the motion under the linear dynamics.[13] However, this investigation is based on a guidance process that operates in a nonlinear relative motion regime and for formations with eccentric Chief orbits. To create the appropriate STM for the AAPF description, the Yamanaka-Ankersen (YA) approximation for the STM is employed. The YA STM is an analytical, linear approximation of the relative motion dynamics in the Hill frame for Chief orbits of any eccentricity.[14] The YA STM was selected because it is more representative of the nonlinear relative motion dynamics than

the CW STM, and is faster to compute than a numerically integrated STM.[14] As is demonstrated in the later simulations, though it is a linear approximation, AAPF guidance using the YA STM successfully guides the spacecraft to their targets under unperturbed as well as perturbed nonlinear orbital dynamics.

Since artificial potential function guidance and, to a lesser extent, adaptive artificial potential function guidance use the distance between the spacecraft and target as the basis for the size of the recommended ΔV maneuvers, APF and AAPF can recommend maneuvers that are not feasible for actual implementation. The incorporation of an approximation of the natural dynamics in the AAPF calculations reduces this effect, but may not eliminate it in every scenario. Capping the size of individual maneuvers in the simulations bounds the upper limit of any impulsive ΔV. For the simulations here, each impulsive ΔV is capped at 0.5 m/sec. The total ΔV along a trajectory is not limited, but each impulsive maneuver is bounded by 0.5 m/sec. Conversely, there is no lower bound on ΔV.

There are some parameters in the APF and AAPF structure that can be selected for tuning. These include k, K, P, and τ. In this investigation, unless otherwise noted, k is set at $1/200$, K is assigned a value of $1/20$, and P is fixed to be:

$$P = \frac{1}{100}\begin{bmatrix} 1 & 0 & 0 \\ 0 & 1 & 0 \\ 0 & 0 & 1 \end{bmatrix}$$

This selection for P sets up a sphere of repulsion with a 10 m radius. The choice of τ impacts the performance of the AAPF guidance algorithm, as demonstrated in Figure 3 and Table 1. These results from several simulations of the AAPF and APF guidance algorithms, with different τ values. All simulations originate with the same initial conditions and the spacecraft are consistently aimed at the same targets. In these simulations, the Chief orbit has a perigee altitude of 1,000 km and an eccentricity of 0.1. In Figure 3, the APF method (which does not employ a look-ahead time, τ) guides the spacecraft more directly toward the target and this APF formulation requires the most ΔV. For the AAPF strategy, as τ increases from $p/6$ to $p/4$–where p is the orbital period of the Chief orbit–the relative path of the spacecraft shifts away from the target initial position as the attractive potential incorporates more of the inherent motion of the Hill frame. This sensitivity to the natural dynamics corresponds to a path that requires less ΔV to reach the target. For these simulations, the lowest ΔV is achieved with a τ value that varies as the trajectory evolves.

Table 1. ΔV for Figure 3

Guidance	τ	ΔV (m/s)	ToF (min)
APF	–	20.38	54.92
AAPF	p/6	9.57	130.17
AAPF	p/5	8.31	173.17
AAPF	p/4	7.68	232.58
AAPF	var	6.58	198.50

In the previous example, an adaptive artificial potential function guidance approach, using a variable τ, results in the least use of ΔV to guide the spacecraft to the target. In this AAPF version, the τ is selected before every maneuver with the following method; first, using Eq. (28) with the Clohessy-Wiltshire STM as the working STM, an initial maneuver cost is calculated, ΔV_0, corresponding to an arbitrary final time, t_f. Then, once again using the CW dynamics, a final maneuver

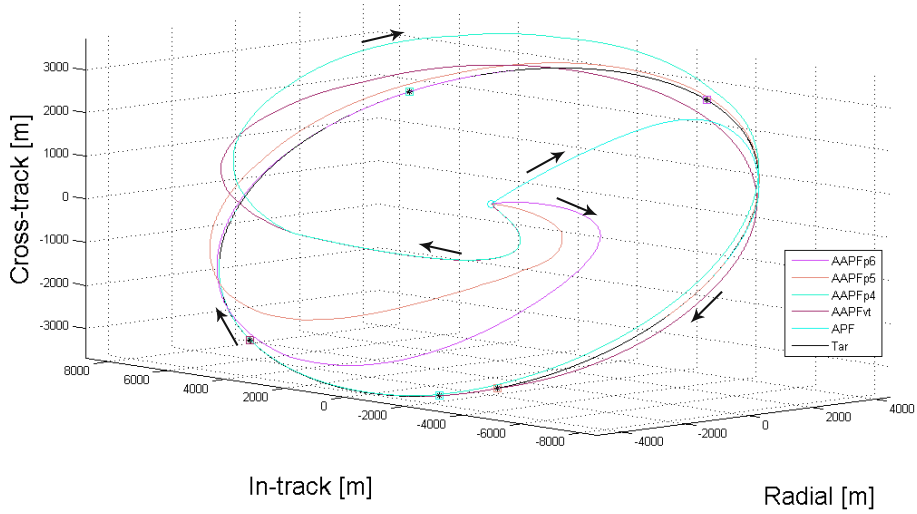

Figure 3. Trajectories in the Hill frame for spacecraft under APF and AAPF with different τ values and their target.

cost, ΔV_f, is computed to match the relative velocities at t_f. Next, the total maneuver cost is calculated: $\Delta V_T = \Delta V_0 + \Delta V_f$. This sequence is accomplished for a series of t_f values between the current time, t, and $t + p/4$. The t_f that corresponds to the lowest ΔV_T value is identified to create the τ to be used in calculating the AAPF for the maneuver thusly: $\tau = t_f - t$. Since these ΔV values are only used for estimation purposes, the CW STM is employed in the τ calculation instead of the YA STM for reasons of computational simplicity. This process for the determination of τ improves the ΔV performance of the AAPF guidance algorithm as is demonstrated in the above example, but is not guaranteed to minimize the cost. Though using the CW equations to model the relative dynamics is computationally efficient, the process still requires more total computational time in comparison to the standard AAPF method since these τ calculations are completed prior to every possible maneuver. For the following demonstrations, unless noted otherwise, all AAPF guidance uses a fixed look-ahead time of $\tau = p/4$. This value may not be optimal for every scenario, but it serves as a reasonable compromise.

ASSIGNMENT

The assignment problem is actually the first problem for the guidance algorithm, that is, n spacecraft must be matched to n targets in the desired formation. There is a benefit, b_{ij}, to matching spacecraft i to target j, and the goal is the assignment that maximizes the total benefit to the formation. The benefit for a particular match is a combination of a number of different factors. For example, certain positions may be pre-specified to be filled by specific spacecraft; as a consequence, there is a greater benefit to that match. If all the spacecraft are interchangeable, the benefit might be based on the propellant required to reach the target, the time of flight, or mission-specific criteria. This guidance formulation uses an auction process to solve the assignment problem. The classic auction algorithm is described and then modified. The modified auction performance is evaluated. In this investigation, all the spacecraft are assumed to be interchangeable, i.e., every position is open to every spacecraft.

Classic Auction Algorithm

The auction algorithm from Bertsekas is based around bidding and increasing prices.[6] As previously noted, there is a benefit, b_{ij}, for matching spacecraft i to target j and each target j has an associated price, p_j. Initially, the targets are all defined with the same price, but the individual prices may increase based on the target desirability. The value of target j to spacecraft i is the benefit minus the price, $b_{ij} - p_j$. The goal for each spacecraft is a match with the target that offers the maximum value. If target j is the best match for spacecraft i, the mathematical expression is:

$$b_{ij} - p_j \geq \underset{k=1,\ldots,n}{max} \{b_{ik} - p_k\} \tag{40}$$

When a spacecraft i is assigned to a target that yields the maximum value, it is "satisfied" and, if all the spacecraft in a formation are sufficiently satisfied, the assignments and target prices are at "equilibrium". This equilibrium assignment supplies the maximum total benefit and solves the assignment problem.

The equilibrium assignment is reached through the auction process. This process can be applied in parallel or serially; initially the serial method is employed, but a true decentralized formation requires the algorithm to be applied on each spacecraft in parallel.[15] Following the method described by Bertsekas, a parameter, ϵ, is introduced that aids the algorithm in avoiding tie bids. Using this parameter, the definition of "satisfaction" is adjusted. The spacecraft i is satisfied with target j if the value is within ϵ of the maximum value:

$$b_{ij} - p_j \geq \underset{k=1,\ldots,n}{max} \{b_{ik} - p_k\} - \epsilon \tag{41}$$

Now the auction is no longer guaranteed to deliver the equilibrium assignment, but the assignment is within ϵ of the equilibrium assignment satisfaction.

The auction process proceeds in "rounds" and, in each round, a different spacecraft bids on targets. Assume that spacecraft i is initially assigned to target k, but target j provides the maximum value. Spacecraft i then switches its assignment to target j and raises the price on target j, p_j, by γ_i. (Whichever spacecraft was previously assigned to target j, is now assigned to target k.) Thus, γ_i is the bid by spacecraft i. The value of this bid is determined by the difference between the maximum and second maximum values for spacecraft i and ϵ:

$$\gamma_i = v_i - w_i + \epsilon \tag{42}$$

Here, v_i is the maximum value for spacecraft i and is defined as:

$$v_i = \underset{k=1,\ldots,n}{max} \{b_{ik} - p_k\} \tag{43}$$

Therefore, v_i is the value of target j for spacecraft i, $v_i = b_{ij} - p_j$. Then, w_i is the second maximum value for spacecraft i and is defined as:

$$w_i = \underset{k=1,\ldots,n,k\neq j}{max} \{b_{ik} - p_k\} \tag{44}$$

In other words w_i is the maximum value for spacecraft i considering all the targets except target j. The introduction of ϵ to the bid ensures that, in the unlikely case where v_i and w_i are equal, the price of target j, p_j, increases by at least ϵ. This inclusion of ϵ is important to ensure that the prices of the targets increase until the (near) equilibrium is achieved. Once target j's price is increased by γ_i, the next spacecraft emerges to participate in the auction. If a spacecraft is satisfied with its current assignment, then no action occurs and the auction continues with the next spacecraft. This process repeats until all the spacecraft are satisfied.

Modified Auction

The auction algorithm is attractive because of its computational simplicity and its success in producing near-equilibrium assignments.[6] The key to a successful auction is assigning the benefits of the target so that an equilibrium assignment corresponds to a desirable formation from the operator viewpoint. In this investigation, the goal of the auction is the combination of assignments that use the least total ΔV for the formation. Given the goal, the auction is restructured to seek a minimum rather than a maximum. The benefits, b_{ij}, as defined in the auction are related to the maneuver ΔV as recommended by the guidance system to deliver spacecraft i to target j. The prices, p_j, corresponding to the targets are initially set equal and rise as the auction progresses. The value of target j to spacecraft i is represented by v_{ij} which is updated as:

$$v_{ij} = b_{ij} + p_j \tag{45}$$

Since the auction seeks a minimum total ΔV, the spacecraft is "satisfied" if its current value is within ϵ of the lowest possible. In other words, spacecraft i is satisfied with target j if:

$$b_{ij} + p_j \leq \underset{k=1,\ldots,n}{min} \{b_{ik} + p_k\} + \epsilon \tag{46}$$

Similar to the classic auction, if the spacecraft is not satisfied with its current assignment, it acquires the target with the lowest value. If spacecraft i is initially assigned to target k and is not satisfied, spacecraft i switches to target j; the spacecraft that was previously assigned to target j now is reassigned to target k. The price of target j is raised by $\gamma_i = w_i - v_{ij} + \epsilon$, where v_{ij} is the lowest possible value for spacecraft i and w_i is the second lowest value. Once again, the slack variable, ϵ, ensures that the price always rises by at least a small amount. Once spacecraft i has completed this process, the auction shifts to the next spacecraft. The auction continues until all spacecraft are satisfied.

Given its importance, the slack variable ϵ is further analyzed. With the implementation described above, Bertsekas introduces the slack ϵ as a tie-breaker, but it can also speed up the auction process by increasing the size of bids.[6] Bertsekas investigates the optimal size of ϵ and determines that, for n members of the auction, the optimal size is $\epsilon < {}^{1}/_{n}$.[6] In this effort, $\epsilon = {}^{1}/_{(n+1)}$. Under this formulation, as n increases ϵ decreases; thus, as n increases, the auction assignment shifts closer to the true equilibrium assignment where all spacecraft are perfectly satisfied.

In this investigation, three methods of assigning benefit, Auc1, Auc2, and Auc3, are considered. Auc1 bases the benefits entirely on the first recommended ΔV maneuvers from the previously described AAPF guidance strategy. Only the first maneuver is actually computed for two reasons: (i) no simulation is required to compute the first maneuver and, thus, the computational load is eased, and (ii) in traditional APF guidance, the first maneuver is the largest and representative of the subsequent path. Auc2 simulates the end-to-end trajectory from spacecraft i to target j using the Yamanaka-Ankersen approximation as the dynamics model and the usual AAPF for guidance, sums the ΔV employed in the simulation and defines it as the benefit, b_{ij}. The use of the Yamanaka-Ankersen approximation avoids numerous numerical simulations within the auction process, while the end-to-end simulation incorporating the maneuvers is a more realistic benefit to enable accurate estimates in the auction process. Auc3 is similar to Auc2, but the algorithm in Auc3 numerically integrates the relative motion equations in its simulations. This expanded numerical integration adds to the computational load on each spacecraft, but supplies the auction with benefits that accurately represent the ΔV cost for the formation reconfiguration maneuver.

To test the performance of each auction method, 14 simulations of reconfiguration maneuvers are designed. The formation sizes range from three to six spacecraft. The spacecraft all originate within 100 m of the Chief origin, while the targets range from 200 m to 1 km in initial separation distance with respect to the Chief. Each auction method creates an assignment and, then, the spacecraft are each guided to their target using the AAPF algorithm. The results for the total formation ΔV from each simulation are displayed in Table 2, along with the number of spacecraft in the formation and the ϵ value for each auction. For evaluation purposes, every combination of spacecraft and target assignment is also simulated for every formation. The lowest total ΔV from all possible combinations appears in the "Best" column. It should be noted that this analysis requires $n!$ simulations for every formations, whereas Auc2 and Auc3 require only n^2 simulations.

Table 2. Auction Comparisons

n	ϵ	Auc1 (m/s)	Auc2 (m/s)	Auc3 (m/s)	Best (m/s)
3	$1/4$	3.1898	2.2088	2.2088	2.2088
4	$1/5$	2.1798	2.1798	2.1798	2.1798
5	$1/6$	3.1581	3.0269	3.0269	2.9353
4	$1/5$	2.1850	1.8289	1.8289	1.8289
6	$1/7$	4.0047	3.8581	3.8581	3.8581
5	$1/6$	3.0673	2.7463	2.7463	2.7463
5	$1/6$	3.1254	2.5841	2.6397	2.5677
3	$1/4$	2.7439	2.7439	2.7439	2.7134
4	$1/5$	2.5187	2.5187	2.4476	2.4476
4	$1/5$	2.1580	2.1580	2.1580	1.9945
3	$1/4$	2.1923	1.6362	1.6362	1.6362
6	$1/7$	2.9724	2.5276	2.5276	2.5276
6	$1/7$	2.7027	2.5912	2.5912	2.5912
6	$1/7$	3.9365	2.5910	2.5910	2.5910

It is apparent in Table 2 that the assignments from Auc1 generally use more total ΔV than those from Auc2 and Auc3. The assignments from Auc2 and Auc3 are virtually identical in their performance. Thus, the Yamanaka-Ankersen approximation very well reflects the results from numerical integration of the relative motion dynamics; the approximation saves on computational requirements. In comparison to the results in the "Best" column, the assignments from Auc2 and Auc3 are all within ϵ of the minimum cost assignments. This result is consistent with Bertsekas's demonstration that the auction assignment is within ϵ, in terms of satisfaction, of the equilibrium assignment.[6] Based on these results, the demonstrations of the complete guidance algorithm employ the Auc2 system of calculating benefits in the modified auction method described in this section to assign targets to the spacecraft.

GUIDANCE ALGORITHM DEMONSTRATIONS

The complete guidance algorithm is demonstrated operating in support of several formation reconfiguration maneuvers. The operator supplies only the initial states of the spacecraft and targets. The auction algorithm then assigns the spacecraft to targets, and each spacecraft is then guided to its target using the AAPF strategy. In all the following examples, the Chief orbit is defined with a perigee altitude of 1,000 km and an eccentricity of 0.1. The AAPF guidance law uses a τ value of

$p/4$ where p is the Chief orbital period, K is set at $1/20$, and P is:

$$P = \frac{1}{100}\begin{bmatrix} 1 & 0 & 0 \\ 0 & 1 & 0 \\ 0 & 0 & 1 \end{bmatrix}$$

The modified auction is employed as described and the evaluation of benefits is accomplished with the Auc2 method. All the simulations (except the last) use the nonlinear equations of orbital relative motion; the last example uses perturbed orbital dynamics to demonstrate the guidance strategy under perturbations.

The trajectories resulting from the first demonstration appear in Figure 4. In this example, four spacecraft originate near the origin of the Hill frame and move into a larger formation. The total ΔV required to configure the formation is 2.37 m/s. In the second demonstration, in Figure 5, the

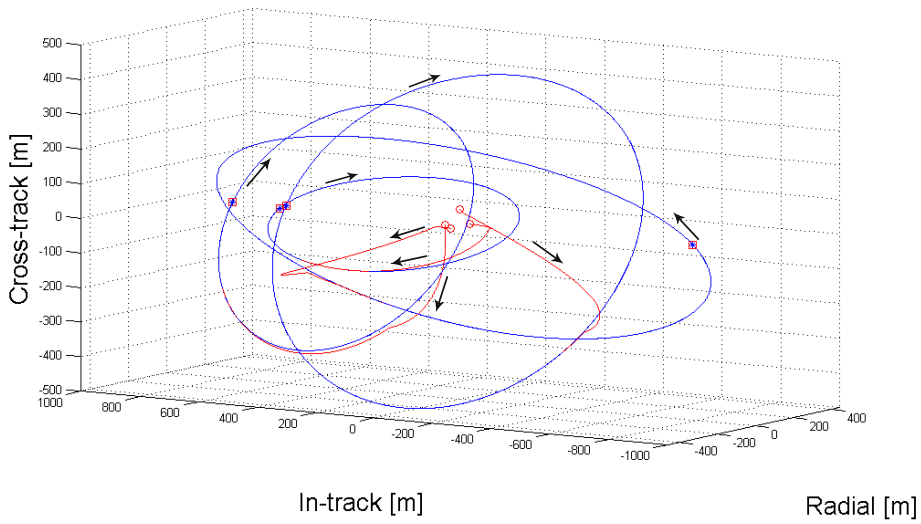

Figure 4. Trajectories in the Hill frame for a reconfiguration maneuver of a formation of 4 spacecraft. The spacecraft trajectories are in red, and the target paths are in blue. The initial spacecraft positions are circles, and the final positions are squares.

four spacecraft start in a smaller arrangement, about 100 m separations between the Chief and other spacecraft in the formation, represented by the black trajectories in the figure; then, the spacecraft move into a larger formation geometry, about 1 km separation, represented by the blue trajectories, with more out of plane motion. The out of plane motion in the Hill frame represents spacecraft with different orbital inclinations relative to the Chief. The total ΔV required by the formation is 6.09 m/s under the new scenario. The third demonstration, which is a simulated phasing maneuver, appears in Figure 6. The five spacecraft are initially positioned in a small formation and trail the reference point in the Hill frame by about 1 km. The initial configuration is transitioned to a larger formation which leads the reference point by about 500 m. The total ΔV necessary to form the new configuration is 8.58 m/s.

The final demonstration, in Figure 7, represents a reconfiguration maneuver under perturbed dynamics. The perturbations include the Earth's J_2 through J_6 zonal harmonics terms, the gravitational forces from the Sun and Moon and solar radiation pressure are also incorporated. Each spacecraft possesses a surface area of 25 m^2, a mass of 200 kg, and $\epsilon_R = 0.22$–where ϵ_R is reflectivity. The equations of motion for this simulation and the natural parameters used in this simulation

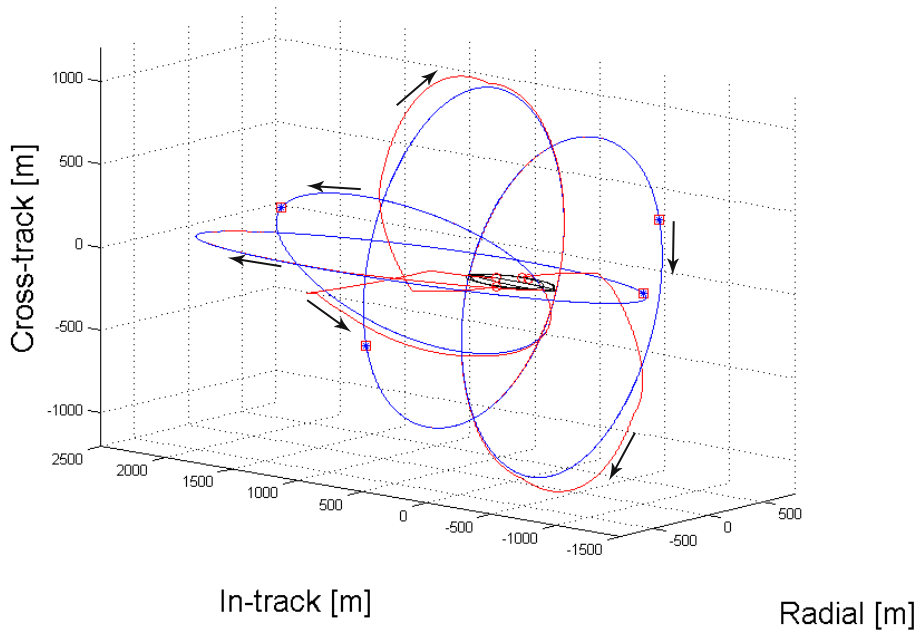

Figure 5. Trajectories in the Hill frame for a reconfiguration maneuver of a formation of 4 spacecraft. The spacecraft trajectories are in red, and the target paths are in blue. The original formation motion is in black. The initial spacecraft positions are circles, and the final positions are squares.

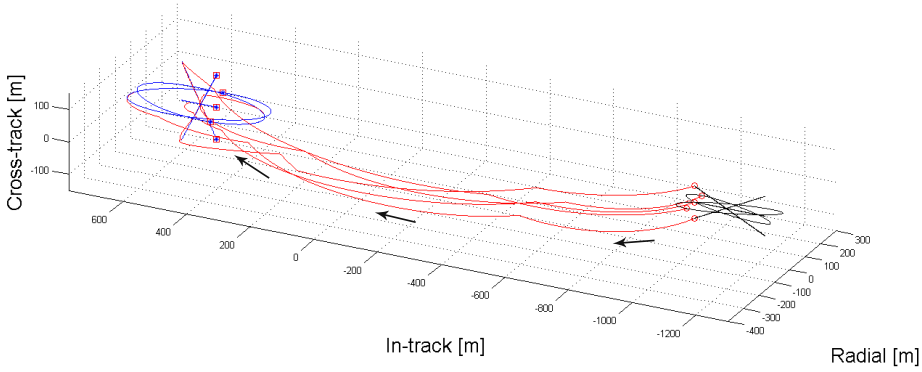

Figure 6. Trajectories in the Hill frame for a reconfiguration maneuver of a formation of 5 spacecraft. The spacecraft trajectories are in red, and the target paths are in blue. The original formation motion is in black. The initial spacecraft positions are circles, and the final positions are squares.

are described by Montenbruck and Gill.[16] In this simulation, the Chief orbit is defined by a perigee altitude of 1,000 km, an eccentricity of 0.1, and an initial inclination of 10 degrees. The total ΔV required by the formation is 2.75 m/s. Note that both the auction and guidance strategy successfully deliver the spacecraft to the final formation in this higher-fidelity dynamical environment.

These demonstrations illustrate the ability of the guidance algorithm to accomplish formation reconfiguration maneuvers in a variety of scenarios. The strategy achieves formations ranging in size from hundreds of meters to several kilometers of separation between the spacecraft. The algorithm can reorient the formation as viewed in the Hill frame while adjusting the formation size. The

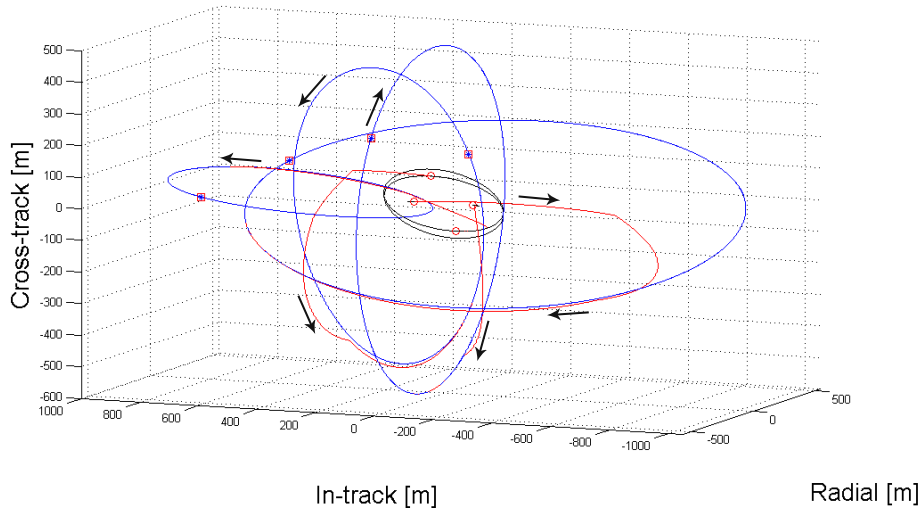

Figure 7. Trajectories in the Hill frame for a reconfiguration maneuver of a formation of 4 spacecraft under perturbed dynamics. The spacecraft trajectories are in red, and the target paths are in blue. The original formation motion is in black. The initial spacecraft positions are circles, and the final positions are squares.

success of this guidance approach in achieving the formation geometry under perturbed dynamics is notable, while the AAPF leverages the Yamanaka-Ankersen STM to create the potential. The general approach is successful and efficient, even under a perturbed Keplerian environment.

CONCLUDING REMARKS

A guidance strategy based on auctions and artificial potential functions for formation reconfiguration maneuvers is introduced. This algorithm is designed for minimal operator input and implementation in nonlinear dynamical regimes. The algorithm solves the joint assignment and delivery problems autonomously and efficiently. It successfully incorporates an auction process to assign the spacecraft to new positions in the formation and then accesses adaptive artificial potential functions to deliver them to the specified targets. In simulations, the operator inputs the desired formation geometry and the guidance algorithm is successful in creating the new formations in a variety of scenarios under nonlinear and perturbed dynamics.

In continuing developments, the guidance algorithm will be tested in increasingly realistic simulations. The algorithm is successful under perturbed dynamics, but future simulations will include uncertainties in the target, obstacle, and spacecraft states to reflect limitations on sensor accuracy. Uncertainties in the thrusting maneuvers will also be included. To address these types of uncertainties and perturbations, a filtering process will be included to the guidance system. More mission specific formation geometries will also be explored to test the algorithm's abilities. Additionally, different propulsion options such as electric or low-thrust can also be incorporated into the spacecraft models.

ACKNOWLEDGMENTS

This material is based on research sponsored by Air Force Research Laboratory (AFRL) under agreement number FA9453-15-1-0306. The U.S. Government is authorized to reproduce and distribute reprints for Governmental purposes notwithstanding any copyright notation thereon.

The views and conclusions contained herein are those of the authors and should not be interpreted as necessarily representing the official policies or endorsements, either expressed or implied, of Air Force Research Laboratory (AFRL) or the U.S. Government.

REFERENCES

[1] "Terrestrial Planet Finder Interferometer," http://exep.jpl.nasa.gov/TPF-I/tpf-I_index.cfm. Accessed: 2015-10-12.

[2] "Darwin Overview," http://www.esa.int/Our_Activities/Space_Science/Darwin_overview. Accessed: 2015-10-12.

[3] M. Martin and M. Stallard, "Distributed Satellite Missions and Technologies—The TechSat 21 Program," *Space Technology Conference and Exposition*, 1999, pp. 28–30.

[4] "About Prisma," http://www.lsespace.com/about-prisma.aspx. Accessed: 2015-10-12.

[5] "The Magnetospheric Multiscale Mission," http://mms.gsfc.nasa.gov/about_mms.html. Accessed: 2015-10-12.

[6] D. P. Bertsekas, "The Auction Algorithm for Assignment and Other Network Flow Problems: A Tutorial," *Interfaces*, Vol. 20, No. 4, 1990, pp. 133–149.

[7] E. Rimon and D. E. Koditschek, "Exact Robot Navigation Using Artificial Potential Functions," *Robotics and Automation, IEEE Transactions on*, Vol. 8, No. 5, 1992, pp. 501–518.

[8] H. Schaub and J. L. Junkins, *Analytical Mechanics of Space Systems 2nd Ed.* Aiaa, 2009.

[9] O. Khatib, "Real-Time Obstacle Avoidance for Manipulators and Mobile Robots," *The international journal of robotics research*, Vol. 5, No. 1, 1986, pp. 90–98.

[10] J. Muñoz, *Rapid Path-Planning Algorithms for Autonomous Proximity Operations of Satellites*. Ph.D. Dissertation, University of Florida, Gainesville, Florida, 2011.

[11] S. S. Ge and Y. J. Cui, "New Potential Functions for Mobile Robot Path Planning," *IEEE Transactions on robotics and automation*, Vol. 16, No. 5, 2000, pp. 615–620.

[12] S. S. Ge and Y. J. Cui, "Dynamic Motion Planning for Mobile Robots Using Potential Field Method," *Autonomous Robots*, Vol. 13, No. 3, 2002, pp. 207–222.

[13] W. H. Clohessy and R. S. Wiltshire, "Terminal Guidance System for Satellite Rendezvous," *Journal of the Aerospace Sciences*, Vol. 27, September 1960, pp. 653–658.

[14] K. Yamanaka and F. Ankersen, "New State Transition Matrix for Relative Motion on an Arbitrary Elliptical Orbit," *Journal of guidance, control, and dynamics*, Vol. 25, No. 1, 2002, pp. 60–66.

[15] D. P. Bertsekas and D. A. Castañon, "Parallel Synchronous and Asynchronous Implementations of the Auction Algorithm," *Parallel Computing*, Vol. 17, No. 6, 1991, pp. 707–732.

[16] O. Montenbruck and E. Gill, *Satellite Orbits: Models, Methods and Applications*. Springer Science & Business Media, 2012.